MODELS FOR SOLAR HEATING OF BUILDINGS

Bernt.Lie@hit.no,*[*] Carlos Pfeiffer, Nils-Olav Skeie
Telemark University College, Porsgrunn, Norway

Hans-Georg Beyer
University of Agder, Grimstad
Norway

ABSTRACT

The standard of living in a country is strongly correlated to the energy consumption, hence a considerable increase in the global energy use is expected. The effects of energy conversion on the climate, e.g. increased CO_2 level, is already observed. Thus it is imperative to base future energy conversion on resources that have negligible climate effects; solar energy is perhaps the most important of such resources.

The general structure of models for solar heating of buildings, with disturbances and relevant sensor technology is described. Simple models of the various parts of the system are developed, and the model is validated through simulation. Requirements for models for on-line control and optimization are discussed. It is noted that ventilation leads to an important energy loss if energy is not recovered by heat integration.

The main contribution in this paper is in putting together submodels from different fields and publications into a relatively complete model structure for control of a residential building. A second contribution is the discussion of key disturbances in the system.

Keywords: Solar heating, Building models, Model efficiency, Control.

INTRODUCTION

The observed increase of greenhouse gases in the atmosphere in tandem with an increase in global temperature, has led to a concern about the temperature development for the rest of the century with the possible consequence of increased ocean level, more violent weather, etc. To counter these predictions, there is an emphasis on reducing the use of fossil fuel and thus stop the increase in CO_2 level of the atmosphere.

Solar energy is a freely available alternative to fossil energy. One possible way to utilize solar energy is to capture the irradiance in a solar collector, and store the energy by heating up water in a storage tank. Such hot water can be used for heating, for showering, etc. The intermittent nature of irradiance is partially handled by such storage of energy, but it is usually necessary to combine solar energy with other energy forms such as electricity or fossil fuel to ensure sufficient availability of power. Because of fluctuations in energy prices (spot marked), it may be possible to take advantage of predictions of irradiance to reduce the energy bill: if we know that tomorrow will be sunny, we can reduce the heating by electricity or fossil fuel – or at least make sure that we use such co-energy forms when their cost is low.

The complexity level of models for solar heating of buildings range from simple models for energy planning over decades to detailed studies of the individual components in such systems. Of particular interest is the study of models suitable for on-line use. Such models should give sufficient information about the dynamics of the system, but should be simple enough to enable advanced on-line control and optimization. Even though detailed models may be necessary in detailed analysis of individual com-

[*]Corresponding author: Phone: +47 3557 5155 Fax: +47 3557 5401 E-mail:bernt.lie@hit.no

ponents, simpler unit models may suffice in a complete system model. This study thus aims at compiling models for the complete system of solar heating of buildings, with the long term goal of developing models that are sufficiently detailed yet sufficiently simple for on-line control and optimization.

For large scale solar collector plants, concentrated solar power systems are used [16], while for domestic heating, flat plate solar collectors or evacuated collectors are cheaper. Here, we focus on domestic heating. The fitting of an industry standard flat plate solar collector model to experimental data is discussed in [12], while [19] and [18] discuss more complex models for transient studies. Both [6] and [8] give useful background in solar radiation and design of such collectors. Models of storage tanks are discussed e.g. in [8], see also [9], [2], and [17]. Software libraries with detailed building models are available, but for control studies, the discussion in [13], [14] is particularly relevant. Disturbances are important in building models. Domestic hot water load profiles are treated in [11]; seasonal variations and optimization is important for design [7] and [3]. Variation in solar irradiance and ambient temperature are typically measured; see e.g. [8]. With respect to on-line use of models, [5] use a simple model of a building together with prediction of outdoor temperature and varying electric spot prices to study possibilities for cost savings through advanced control, with emphasis on efficient algorithms, while [10] and [15] discuss the use of Model Predictive Control of a system for thermal capturing of solar energy with auxiliary energy supply.

The paper is organized as follows. First, a description of the system with solar heating, storage tank and building is given, with some background information. Next, a simple mathematical model is presented. Then, operational conditions are given, and the model is verified through simulations. Finally, some conclusions are drawn.

SYSTEM DESCRIPTION

System elements

A system for mixed solar and electric (auxiliary) heating of a domestic building is depicted in Figure 1.

The reason for introducing heat exchangers to separate the fluids of the collector circuit and the heating

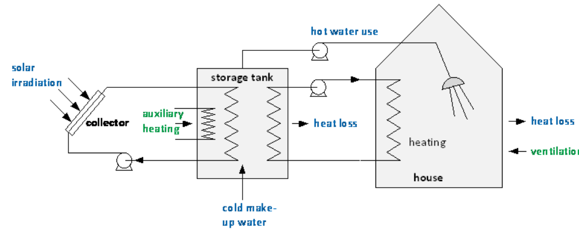

Figure 1: Blue font indicates disturbance variable, while green font indicates control variable. Heat losses are due to temperature differences to ambient temperatures. The storage tank is assumed to be instantly re-filled with cold make-up water, which may have a varying temperature.

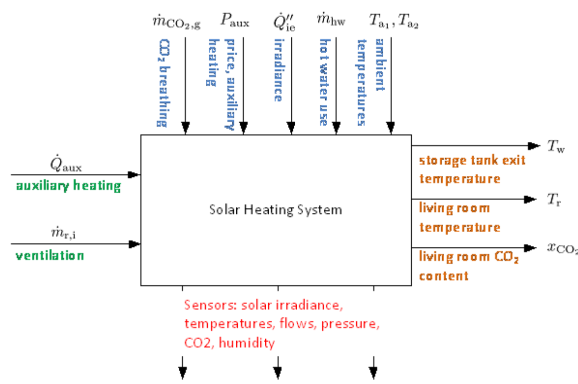

Figure 2: Functional description of the solar heating system with auxiliary heating input.

circuit from the utility hot water of the storage tank, is to allow for use of anti freeze and algae reducing components in these circuits.

Functional description

From a system theoretic point of view, it is useful to present the system as a block diagram with inputs and outputs — inputs and outputs will vary with time; Figure 2 illustrates this causal relationship with disturbances on the top of the block, control inputs (manipulating inputs) at the left side, while performance outputs (orange) are shown on the right side of the system block and available sensor signals (red) at the bottom of the block.

Sensors for buildings

A measurement system is needed to measure or estimate the sun irradiance and several parameters inside the house. In addition, the atmospheric pressure should be measured.

Solar irradiance

The most common sensor device is the pyranometer. The pyranometer measures the solar irradiance flux density $\left(\mathrm{W}/\mathrm{m}^2\right)$ on a planar surface over a 180 degree field of view. The cost and size of pyranometers may be an disadvantage, other options for such a device can be solar cell, photo diode, photo transistor, or light dependent resistor (LDR).

The solar spectrum is dominated by the following wavelengths: ultraviolet $(300-400\,\mathrm{nm})$, visible $(400-700\,\mathrm{nm})$, and near infrared $(700-2500\,\mathrm{nm})$. A pyranometer is able to capture most of the solar spectrum, while the other sensor types capture the visible part.

The output from a solar cell is a voltage proportional to the light intensity. The output from a photo diode and photo transistor is a small variation in current; an electronic circuit is needed to convert this to an output voltage proportional to the light intensity. The output from an LDR is also current; an extra resistor suffices to have an output voltage proportional with the light intensity. These sensor devices are easy to integrate into a measurement system. A model must however be added to be able to estimate the sun irradiance from these sensor devices.

Other sensors

Other sensor devices needed for buildings include sensors for temperature, humidity, CO_2, flow, and pressure.

Several types of temperature sensor devices exist, both contact and non-contact types. Small, contact type sensor devices based on semiconductors are suitable for temperature measurement. The output is voltage, proportional to the temperature in the range $[-20\,^\circ\mathrm{C}, +60\,^\circ\mathrm{C}]$, and with an accuracy of ± 1 °C. These devices can be connected directly to a measurement system. If a higher accuracy is needed in a small sized sensor, then a resistance temperature detector (RTD) should be considered. The accuracy of these devices can be ± 0.2 °C. However, these sensor devices will require an additional electronic circuit for connection to a measurement system.

Humidity and CO_2 measures are needed to assess the quality of the air inside the house, depending on the ventilation system. These sensor devices can also be of small size, however the cost may be a little higher then the other sensor devices in use. These sensor devices can normally be connected directly to a measurement system.

Flow of water can be measured by using a Coriolis mass flow meter or a magnetic flow meter. In principle, differential pressure sensors can also be used, but these require a relatively large pressure drop — which is unwanted. The most common flow meter is thus the magnetic flow meter, suitable for a wide range of pipe sizes. Flow meters normally use a digital connection with a standard protocol for connection to a measurement system. The cost of a Coriolis mass flow meter is higher than for a magnetic flow meter.

An absolute pressure sensor can be used to measure the atmospheric pressure. It may be useful to have pressure sensors inside the house as well; this will however require absolute pressure sensors of high accuracy.

Logging

The measurement system needs to include a preprocessing and a logging module, where the possibility of wireless connection between sensors and these modules is desirable. The preprocessing unit should take care of sensor errors and filtering (low pass filtering) of the measured values. The module may also include a check for outliers and early warnings. The logging module should be able to log the sensor value, the time stamp and the sensor status. The logging format can be either a set of text files such as a CSV format, or a database such as SQL or OPC.

On notation

In mathematical physics, *flux* is used to denote the flow of an *extensive* variable, while *flux density* is used to denote flux per unit area. In the field of *transport phenomena*, on the other hand, flux normally denotes the flow per unit area. Here, we will adopt the convention from transport phenomena.

It is relatively common to use a dot notation to indicate the flow of an extensive quantity, e.g. $\dot{m}$ implies mass flow where m is the extensive quantity *mass*; $\dot{Q}$ denotes heat flow where Q is the standard thermodynamics symbol for heat. Furthermore, we will use a prime notation do indicate per unit length, thus double prime denotes per unit area. It follows that $\dot{Q}''$

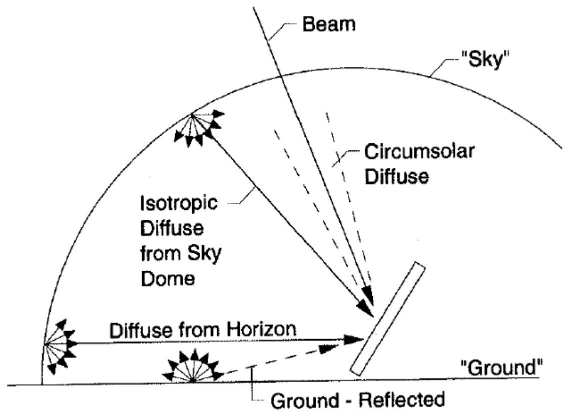

Figure 3: Beam, diffuse, and ground-reflected radiation on a tilted surface. From [6], fig. 1.16.1, p. 91.

denotes heat flux (e.g. unit W/m^2).

Fundamentals of radiation

Radiation emitted from a *black body* follows Planck's law with a *spectral heat flux* $\dot{Q}''_{\mathrm{b},\lambda}$ (monochromatic, at wavelength λ); integrated over all wavelengths the *extraterrestrial*[1] flux at the entrance to the atmosphere is $\dot{Q}''^{,\circ}_{\mathrm{x}} = 1360\,\mathrm{W}/\mathrm{m}^2$ on average, varying slightly with the varying sun-earth distance. The atmosphere has a profound effect on solar radiation. The irradiance that hits a solar collector will thus consist of direct *beam* radiation, diffuse radiation from the "sky", but also of reflected radiation from the ground. In summary, the position on earth of the solar collector will reduce the local extraterrestrial irradiance from $\dot{Q}''^{,\circ}_{\mathrm{x}}$, and because of the rotation of the earth, the irradiance will vary diurnally. Clouds, etc. will also reduce the available irradiance. Figure 3 illustrates how the various radiation components hit a tilted collector.

The glazing on solar collectors have a transmittance that varies with the wavelength (Planck's law): the radiation emitted from the sun with a surface temperature of $T_\sigma = 6000\,\mathrm{K}$ will mainly pass through the glazing, while the radiation emitted from the collector surface at a temperature of perhaps 400 K will have a shifted wavelength distribution and will be blocked. This effect is very important for the efficiency of solar collectors.

[1] Extraterrestrial implies just outside of the earth's atmosphere, with basically vacuum between the sun and the extraterrestrial surface.

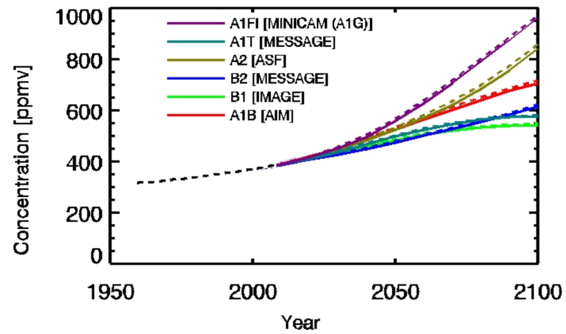

Figure 4: Atmospheric CO2 concentrations as observed at Mauna Loa from 1958 to 2008 (black dashed line) and projected under the 6 SRES marker and illustrative scenarios. Taken from www.ipcc-data.org/observ/ddc_co2.html.

Operational requirements

In general, the temperature comfort zone is around 20 °C, depending somewhat on humidity. In a working environment, 18–20 °C seems to be common. During a summer day, higher temperatures are acceptable to avoid excessive cooling expenses. During night/sleep, lower temperatures are preferable.

Acceptable levels of CO_2 in populated rooms are[2] $x_{CO_2} \leq 600$ ppm. At levels in the range $x_{CO_2} \in [600, 1000]$ ppm, stiffness and odor will be observed.[3] Because breathing produces CO_2, ventilation is necessary; a typical requirement is to replace the air in a room 4 times per hour — the origin of this requirement is to satisfy the limit on x_{CO_2} level in the room. The CO_2 level of the atmosphere is currently[4] at a mole fraction of $x_{CO_2} = 401.3$ ppm $= 401.3 \times 10^{-6}$. Predictions of CO_2 levels are published by IPCC[5], and vary considerably depending on underlying assumptions and models, Figure 4. If the atmospheric CO_2 level increases as indicated in Figure 4, this may have a dramatic effect on the ventilation rate in the next few decades.

Hot water in storage tanks typically is required to have a temperature $\geq$ 55–60 °C to avoid problems with Legionella bacteria, etc.; higher temperatures up to 90 °C is relatively common. Such hot water

[2] www.engineeringtoolbox.com/co2-comfort-level-d_1024.htmlwww.engineeringtoolbox.com/co2-comfort-level-d_1024.html

[3] ASHRAE and OSHAE standards are 1000 ppm.

[4] `http://co2now.org/`

[5] `www.ipcc-data.org/observ/ddc_co2.html`

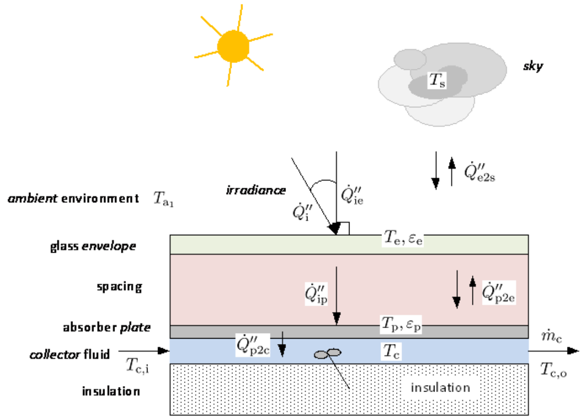

Figure 5: Sketch of collector system with some notation.

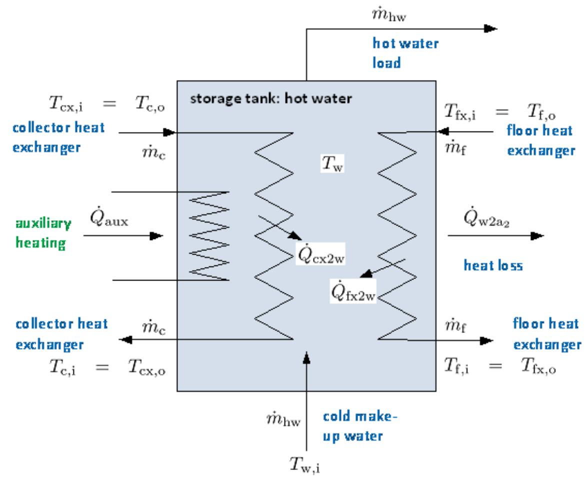

Figure 6: Sketch of storage tank.

is used for under floor heating (UFH), showering, etc. Mixing with cold water is common to reduce the temperature to usable levels. The liquid circulating in solar collectors may need anti-freeze components in Nordic countries, thus it is common to have a closed circuit for the solar collector fluid with heat exchange to the storage tank. Similarly, it is common to have closed circuits for UFH, with heat exchange to the storage tank.

MODEL DESCRIPTION

Collector system

The collector system with some notation is depicted in Figure 5. Models for the collector system ranges from full scale distributed CFD models to 1D and 0D models. As part of these models, it is necessary to describe the irradiance, and in particular how clouds, pollution, etc. reduces the theoretically available irradiance given by a *clearness index* $k_c < 1$. For design purposes, it is common to use a simplified model of the heat flow from the absorber plate to the collector fluid, $\dot{Q}_{p2c}$,

$$\dot{Q}_{p2c} = \eta_{e2c} A_e \dot{Q}''_{ie}$$

where A_e is the efficient surface of the glass envelope, $\dot{Q}''_{ie}$ is the solar irradiance entering perpendicular to the glass envelope, and η_{e2c} is the collector efficiency described as

$$\eta_{e2c} = \eta_{e2c,0} - a_1 \frac{\Delta T_c}{\dot{Q}''_{ie}} - a_2 \frac{\Delta T_c^2}{\dot{Q}''_{ie}},$$

with parameters defining the collector given by $\eta_{e2c,0}, a_1, a_2$. $\Delta T_c \triangleq \bar{T}_c - T_{a_1}$ is the difference between the temperature of the collector fluid and the ambient temperature; in Europe it is common to let $\bar{T}_c$ be the average of the influx and efflux temperatures of the collector fluid, $T_{c,i}$ and $T_{c,o}$. This model is combined with a steady state energy balance for the collector fluid, leading to

$$\dot{m}_c \hat{c}_{p,c} \left(T_{c,o} - T_{c,i} \right) = \dot{Q}_{p2c}$$

A problem which is sometimes not explicitly stated for this simple model is that the efficiency may go to $\pm\infty$ during the night ($\dot{Q}''_{ie} \to 0$); it is also possible that η_{e2c} becomes negative in some operating regimes. To make the model physically realistic, one may set $\dot{m}_c$ to zero when $\eta_{e2c} < 0$ or $\dot{Q}''_{ie} \to 0$.

Storage tank

A storage tank with heat exchangers is depicted in Figure 6. In reality, storage tanks are more or less stratified, i.e. the temperature varies from a low temperature at the bottom to a high temperature at the top, and it is thermodynamically beneficial to operate the system in such a way that water at different temperatures is not mixed: mixing leads to entropy increase. Stratification has been modeled in various ways, from fully distributed CFD models to 1D plug flow models to a sequence of 0D models.

Here we assume that the collector heat exchanger, the floor heat exchanger, and the water storage tank all are well mixed. The storage tank may have heat loss to the ambient temperature T_{a_2} of the room where the storage tank is placed.

An alternative could have been a main storage tank heated by the solar collector and used for under floor heating, followed by a secondary tank for hot water consumption operating at a higher temperature, with influx from the main storage tank and with auxiliary heating. However, here we use a 0d model of a single storage tank. Collector fluid in heat exchanger:

$$m_{\mathrm{cx}}\hat{c}_{\mathrm{p,cx}}\frac{dT_{\mathrm{cx}}}{dt} = \dot{m}_{\mathrm{c}}\hat{c}_{\mathrm{p,cx}}\left(T_{\mathrm{c}} - T_{\mathrm{cx}}\right) - UA|_{\mathrm{cx2w}}\left(T_{\mathrm{cx}} - T_{\mathrm{w}}\right),$$

floor fluid in heat exchanger:

$$m_{\mathrm{fx}}\hat{c}_{\mathrm{p,fx}}\frac{dT_{\mathrm{fx}}}{dt} = \dot{m}_{\mathrm{f}}\hat{c}_{\mathrm{p,cfx}}\left(T_{\mathrm{f}} - T_{\mathrm{fx}}\right) - UA|_{\mathrm{fx2w}}\left(T_{\mathrm{fx}} - T_{\mathrm{w}}\right),$$

the storage tank itself:

$$\begin{aligned} m_{\mathrm{w}}\hat{c}_{\mathrm{p,w}}\frac{dT_{\mathrm{w}}}{dt} &= \dot{m}_{\mathrm{hw}}\hat{c}_{\mathrm{p,w}}\left(T_{\mathrm{w,i}} - T_{\mathrm{w}}\right) \\ &+ UA|_{\mathrm{cx2w}}\left(T_{\mathrm{cx}} - T_{\mathrm{w}}\right) \\ &+ UA|_{\mathrm{fx2w}}\left(T_{\mathrm{fx}} - T_{\mathrm{w}}\right) \\ &- UA|_{\mathrm{w2a_2}}\left(T_{\mathrm{w}} - T_{\mathrm{a_2}}\right) + \dot{Q}_{\mathrm{aux}}. \end{aligned}$$

Building model

We consider a building as proposed in [5], with slight modifications[6]. Their building is a single room with floor heating, with ventilation, and with occupants breathing CO_2 at a given rate. They have additional electric heating; here, this additional heating is added as auxiliary heat to the storage tank. Furthermore, they neglect the inertia of heating the floor; this inertia is added here. To this end, Figure 7 illustrates the parts of the domestic building. Assuming perfectly mixed volumes, we find for the floor fluid:

$$m_{\mathrm{f}}\hat{c}_{\mathrm{p,f}}\frac{dT_{\mathrm{f}}}{dt} = \dot{m}_{\mathrm{f}}\hat{c}_{\mathrm{p,f}}\left(T_{\mathrm{fx}} - T_{\mathrm{f}}\right) - UA|_{\mathrm{f2m}}\left(T_{\mathrm{f}} - T_{\mathrm{m}}\right),$$

floor mass:

$$m_{\mathrm{m}}\hat{c}_{\mathrm{p,m}}\frac{dT_{\mathrm{m}}}{dt} = -UA|_{\mathrm{m2r}}\left(T_{\mathrm{m}} - T_{\mathrm{r}}\right) + UA|_{\mathrm{f2m}}\left(T_{\mathrm{f}} - T_{\mathrm{m}}\right)$$

air temperature:

$$\begin{aligned} m_{\mathrm{r}}\hat{c}_{\mathrm{p,r}}\frac{dT_{\mathrm{r}}}{dt} &= \dot{m}_{\mathrm{r,i}}\hat{c}_{\mathrm{p,r}}\left(T_{\mathrm{a_1}} - T_{\mathrm{r}}\right) + UA|_{\mathrm{m2r}}\left(T_{\mathrm{m}} - T_{\mathrm{r}}\right) \\ &- UA|_{\mathrm{r2a_1}}\left(T_{\mathrm{r}} - T_{\mathrm{a_1}}\right), \end{aligned}$$

[6]The notation is aligned with the notation in this document.

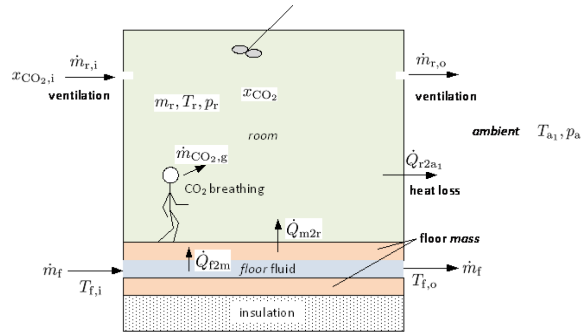

Figure 7: Sketch of domestic building; modification of description in [5].

air mass:

$$\frac{dm_{\mathrm{r}}}{dt} = \dot{m}_{\mathrm{r,i}} - k_{\mathrm{r}}\left(\frac{m_{\mathrm{r}}}{M_{\mathrm{r}}}\frac{RT_{\mathrm{r}}}{V_{\mathrm{r}}} - p_{\mathrm{a}}\right),$$

CO_2 fraction

$$\frac{dx_{\mathrm{CO_2}}}{dt} = \frac{\dot{m}_{\mathrm{r,i}}}{m_{\mathrm{r}}}\left(x_{\mathrm{CO_2,i}} - x_{\mathrm{CO_2}}\right) + \frac{\dot{m}_{\mathrm{CO_2,g}}}{m_{\mathrm{r}}}.$$

Model parameters

The parameters of the model are given in Table 1.

SIMULATION OF MODEL

Disturbance description

The following disturbances are involved in the model, Figure 2.

Hot water load

In [8], it is suggested that the daily consumption of hot water is 30–60 liters per person. A coarse approximation of the domestic hot water consumption (DHWC) distribution of [4] is given in Table 2.
If measurements or better predictions are not available, this distribution can be repeated perpetually in simulations.

Ambient conditions

Ambient temperature $T_{\mathrm{a_1}}$ (out-door temperature) as measured in our case study, [1], is shown in Figure 8. A typical value for the ambient temperature for the hot water storage tank might be $T_{\mathrm{a_2}} = 5\,^{\circ}\mathrm{C}$.

Table 1: Parameters for solar heating system.

Parameter	Value	Unit
a_1	3.83×10^{-3}	$\frac{\mathrm{kW}}{\mathrm{K\,m^2}}$
a_2	6.5×10^{-6}	$\frac{\mathrm{kW}}{\mathrm{K^2 m^2}}$
A_e	$3 \times 1.5 \cdot N_\mathrm{pers}$	m^2
A_r	25	m^2
A_rx	$4 \cdot h_\mathrm{r} \sqrt{A_\mathrm{r}} + A_\mathrm{r}$	m^2
$\hat{c}_\mathrm{pf}$	3.5	$\frac{\mathrm{kJ}}{\mathrm{kg\,K}}$
$\hat{c}_\mathrm{pw}$	4.19	$\frac{\mathrm{kJ}}{\mathrm{kg\,K}}$
$\hat{c}_\mathrm{pm}$	0.63	$\frac{\mathrm{kJ}}{\mathrm{kg}}$
$\hat{c}_\mathrm{pr}$	1.005	$\frac{\mathrm{kJ}}{\mathrm{kg\,K}}$
h_r	2.5	m
k_r	$100 \cdot \frac{1}{1.01 \times 10^5}$	$\frac{\mathrm{kg}}{\mathrm{s\,Pa}}$
ℓ_cx	30	m
ℓ_f	100	m
ℓ_fx	30	m
m_cx	$\rho_\mathrm{w} \cdot \pi r_\mathrm{p}^2 \cdot \ell_\mathrm{cx}$	kg
m_f	$\rho_\mathrm{w} \cdot \pi r_\mathrm{p}^2 \cdot \ell_\mathrm{f}$	kg
m_fx	$\rho_\mathrm{w} \cdot \pi r_\mathrm{p}^2 \cdot \ell_\mathrm{fx}$	kg
m_m	3000	kg
m_w	$60 \cdot N_\mathrm{pers}$	kg
M_r	29	$\frac{\mathrm{kg}}{\mathrm{kmol}}$
N_pers	2	–
r_p	$\frac{13}{2} \times 10^{-3}$	m
R	8.31×10^3	$\frac{\mathrm{J}}{\mathrm{kmol\,K}}$
U_p	0.25	$\frac{\mathrm{kW}}{\mathrm{m^2 K}}$
$UA\vert_\mathrm{cx2w}$	$U_\mathrm{p} \cdot 2\pi r_\mathrm{p} \cdot \ell_\mathrm{cx}$	$\frac{\mathrm{kW}}{\mathrm{K}}$
$UA\vert_\mathrm{f2m}$	$U_\mathrm{p} \cdot 2\pi r_\mathrm{p} \cdot \ell_\mathrm{f}$	$\frac{\mathrm{kW}}{\mathrm{K}}$
$UA\vert_\mathrm{fx2w}$	$U_\mathrm{p} \cdot 2\pi r_\mathrm{p} \cdot \ell_\mathrm{fx}$	$\frac{\mathrm{kW}}{\mathrm{K}}$
$UA\vert_\mathrm{m2r}$	$10 \times 10^{-3} \cdot A_\mathrm{r}$	$\frac{\mathrm{kW}}{\mathrm{K}}$
$UA\vert_\mathrm{r2a_1}$	$0.4 \times 10^{-3} \cdot A_\mathrm{rx}$	$\frac{\mathrm{kW}}{\mathrm{K}}$
$UA\vert_\mathrm{w2a_2}$	$0.5 \times 10^{-3} \cdot 6 \cdot \left(\sqrt[3]{\frac{m_\mathrm{w}}{\rho_\mathrm{w}}}\right)^2$	$\frac{\mathrm{kW}}{\mathrm{K}}$
V_r	$25 \cdot 2.5$	m^3
$\eta_\mathrm{e2c,0}$	0.719, $[0.75, 0.85]$	–
ρ_f	1060	kg/m^3
ρ_w	10^3	kg/m^3

Table 2: Typical DHWC (Domestic Hot Water Consumption) distribution over one day, in %.

Hour	DHWC	Hour	DHWC	Hour	DHWC
00–01	1.4	08–09	11.2	16–17	5.1
01–02	0.70	09–10	10.3	17–18	7.9
02–03	0.23	10–11	4.7	18–19	6.5
03–04	0.47	11–12	3.7	19–20	5.1
04–05	0.47	12–13	2.8	20–21	2.8
05–06	0.23	13–14	2.3	21–22	3.3
06–07	6.5	14–15	3.3	22–23	3.3
07–08	10.7	15–16	3.7	23–24	3.3

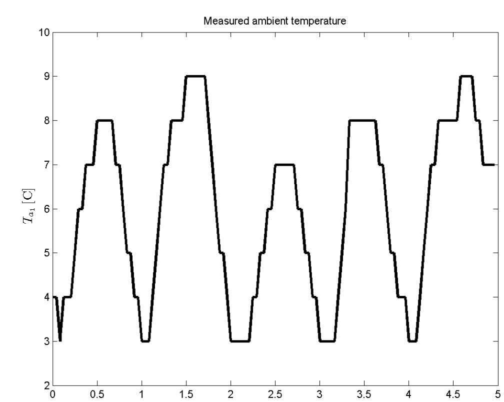

Figure 8: Measured ambient temperature T_{a_1} during five days.

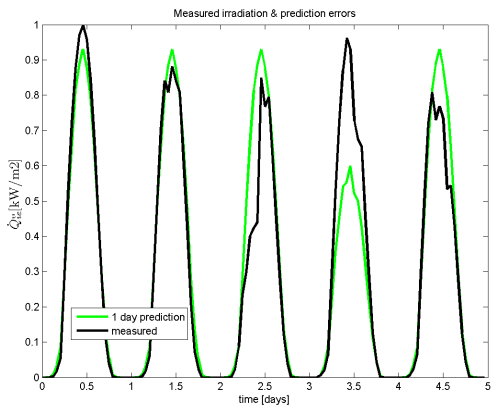

Figure 9: Measured irradiance $\dot{Q}''_{\mathrm{ie}}$ over five days with one-day-ahead prediction.

Solar irradiance

Measured irradiance $\dot{Q}''_{\mathrm{ie}}$ together with prediction error, [1], is displayed in Figure 9.

CO_2 production

In the literature, a typical breathing rate is $1\,\mathrm{kg}/\mathrm{d}$ per person.

Operating conditions

Nominal operating conditions of the system are given in Table 3.

Implementation details

The differential equations are solved using MATLAB, with the `ode15s` ODE solver. The code is divided into a main script file that imports data, runs the simulations and presents results in figures, a script file defining model parameters and operating conditions, and a function file that describes the model/differential equations. Ambient temperature ($T_{\mathrm{a},1}$) and solar irradiance ($\dot{Q}''_{\mathrm{ie}}$) recorded over a period of 30 days in Kristiansand, Southern Norway, are imported from a `.mat` file. The thermostat controller requires an initial value for its state.

Model verification

Using the disturbances from the previous section, the system temperatures for the first 5 days of simulation are depicted in Figure 10. Heat flows in the system are depicted in Figure 11. Collector effi-

Table 3: Nominal operating conditions of the solar heat collector system.

Quantity	Value	Unit
$\dot{Q}_{\mathrm{aux}}$	0	kW
$\dot{m}_{\mathrm{r,i}}$	$\frac{4 \cdot m_{\mathrm{r}}(0)}{3600}$	kg / s
T_{a_1}	10	°C
T_{a_2}	5	°C
$T_{\mathrm{w,i}}$	5	°C
$\dot{m}_{\mathrm{hw}}$	$\frac{50}{24 \cdot 3600} N_{\mathrm{pers}}$	kg / s
$\dot{m}_{\mathrm{c}}$	$\frac{2 \times 10^3}{3600}$	kg / s
$\dot{m}_{\mathrm{f}}$	$\frac{150}{3600}$	kg / s
$\dot{Q}''_{\mathrm{ie}}$	0.5	kW/m^2
$\dot{m}_{\mathrm{CO_2,g}}$	$\frac{1}{24 \cdot 3600} N_{\mathrm{pers}}$	kg / s
$x_{\mathrm{CO_2,i}}$	400×10^{-6}	–
p_{a}	1.01×10^5	Pa
P_{aux}	1	\$/kWh
$T_{\mathrm{cx}}(0)$	44.326	°C
$T_{\mathrm{fx}}(0)$	41.508	°C
$T_{\mathrm{w}}(0)$	48.78	°C
$T_{\mathrm{f}}(0)$	26.3	°C
$T_{\mathrm{m}}(0)$	24.15	°C
$T_{\mathrm{r}}(0)$	18.563	°C
$m_{\mathrm{r}}(0)$	75.584	kg
$x_{\mathrm{CO_2}}(0)$	660.42×10^{-6}	–

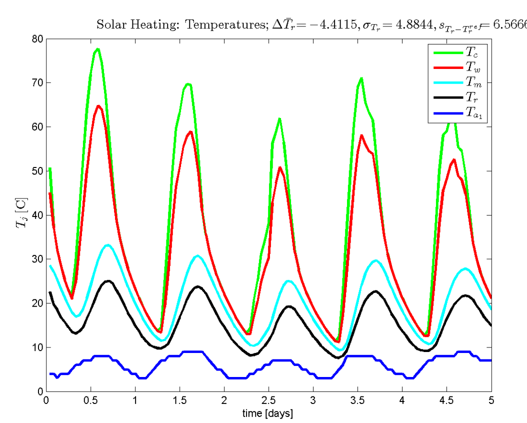

Figure 10: Temperatures at various positions in the system with realistic disturbance inputs.

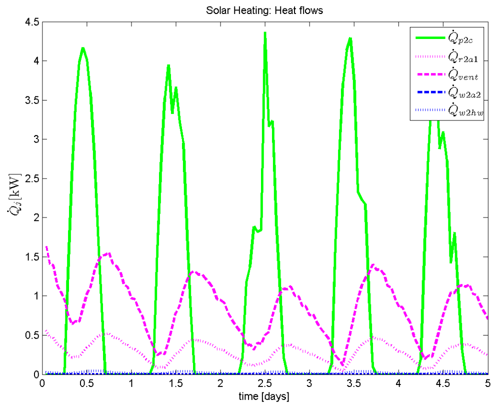

Figure 11: Heat flows at various positions in the system with realistic disturbance inputs.

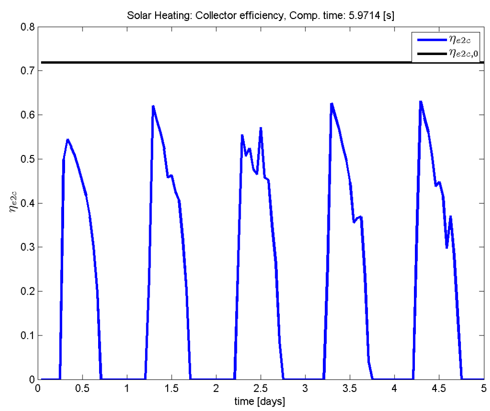

Figure 12: Collector efficiency in the system with realistic disturbance inputs.

ciency in the system is depicted in Figure 12. The results of Figure 12 confirm the importance of modifying the collector model to avoid negative efficiency.

In a second simulation, a *thermostat controller* is used with room temperature setpoint of $T_r^{\mathrm{ref}} = 20\,^\circ\mathrm{C}$. The temperatures for the first 5 days of simulation (simulation time $\propto 10\,\mathrm{s}$) are depicted in Figure 13. The auxiliary heat flow is depicted in Figure 14. Heat flows in the system are depicted in Figure 15.

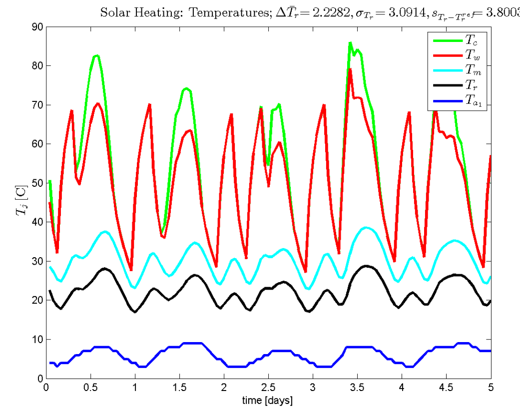

Figure 13: Temperatures at various positions in the system using thermostat controller.

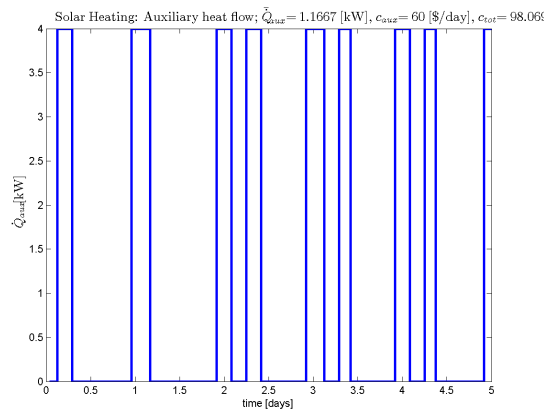

Figure 14: Auxiliary heat input to storage tank using thermostat controller.

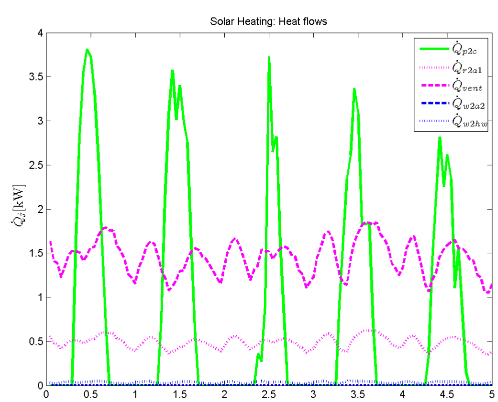

Figure 15: Heat flows at various positions in the system using thermostat controller.

Discussion

The simulations, Figures 10–15, give results that seem to be reasonable from a physical perspective: Temperature levels decrease from that of the collector fluid to that of the ambient temperature (Figures

10, 13), the heat flows seem reasonable (Figures 11, 15), the collector efficiency is as expected (Figure 12), and the auxiliary heat input appears to come into use when the solar irradiance is reduced (Figure 14). These results verify that the model has a sound physical structure. In order to *validate* the model, it would be necessary to compare the model with experimental data, and possibly to tune the model and possibly change its complexity.

The model that has been used for the collector is relatively simple. The reason for this is that only the total forecast $\dot{Q}''_{\mathrm{ie}}$ was available, and not beam irradiance, etc. (Figure 3). Also, the model for the water storage system is simple — too simple to be realistic, which is seen in that the temperature is lower than one would observe in reality. A model that better captures the stratification would improve the overall model; this could perhaps be achieved by using a 2–3 compartment description of the storage tank. Also, the model for the under floor heating (UFH) is somewhat simple, and should be improved. Other heating facilities should perhaps be introduced, e.g. a radiator. The model for the room/building itself is somewhat simple; it would be of interest to consider a building with more than one room, and somewhat more realistic heat transport through walls, etc. Finally, the description of the ventilation system is too simple: modern buildings normally have some sort of heat integration/heat recovery in the ventilation system. In the simulations here, no heat integration is used for the ventilation, and the result is that the heat loss through ventilation (e.g. Figure 15) is the dominating heat loss. This heat loss through ventilation is the reason for the relatively large amplitudes in the temperatures (e.g. Figure 13 except ambient temperature); heat integration would dampen these variations. Also, the IPCC forecasts of future atmospheric CO_2 concentrations indicates the importance of heat integration in the ventilation system.

The heat transfer coefficients that have been used are constants. In reality, heat transfer will vary with flow rates of liquid, etc. Correlations for heat transfer coefficients would also improve the model.

Finally, it is observed that although MATLAB is good for testing prototypes of models, it would be more efficient to build up a library of unit operations which is possible in e.g. Modelica: this would make it much easier to change the topology of the system. Building libraries exist for Modelica, but in this study the emphasis has been on testing models that are suitable for control studies.

CONCLUSIONS

This paper discusses the structure of models for solar heating of buildings applied for on-line control and optimization, with varying levels of detail. A simple model is developed and verified through simulations without and with auxiliary heating of the storage tank. Of particular interest is that the heat loss through ventilation is considerable; this also leads to a relatively large variation in room temperature. The main contribution is in putting together submodels from different fields and publications into a relatively complete model structure for control of a residential building. A second contribution is the discussion of key disturbances in the system.

Future work will consider (i) the detail level of solar collector models, (ii) the detail level of storage tank models, (iii) the detail level of buildings with improved description of under floor heating, possibly with more rooms, and with energy recovery of the ventilated air. Such more complex models will benefit from the use of modern modeling languages, e.g. Modelica. It is of interest to validate the models further against measurements. The main application for the complete system model will be control and on-line optimization.

REFERENCES

[1] Arachchige, D.D.K. (2014). *An Approach to Day Ahead Forecasting of Solar Irradiance with an Application to Energy Gain in Solar Thermal Collectors*. M.Sc. thesis, University of Agder, Faculty of Engineering and Science, Grimstad.

[2] Bayón, R., and Rojas, E. (2013). “Simulation of thermocline storage for solar thermal power plants: From dimensionless results to prototypes and real-size tanks”. *International Journal of Heat and Mass Transfer*, **Vol. 60**, pp. 713–721. http://dx.doi.org/10.1016/j.ijheatmasstransfer.2013.01.047

[3] Cheng Hin, J.N., and Zmeureanu, R. (2014). "Optimization of a residential solar combisystem for minimum life cycle cost, energy use and exergy destroyed". Solar Energy, **Vol. 100**, pp. 102–113.

[4] Defra (2008). *Measurement of Domestic Hot Water Consumption in Dwellings*. Department for Environment, Food and Rural Affairs (Defra), UK.

[5] de Oliveira , V., Jäschke, J., and Skogestad, S. (2013). "Dynamic online optimization of a house heating system in a fluctuating energy price scenario". Preprints of the 10th IFAC International Symposium on Dynamics and Control of Process Systems, The International Federation of Automatic Control, December 18-20, 2013, Mumbai, India, pp. 463—468.

[6] Duffie, J.A., and Beckman, W.A. (2013). *Solar Engineering of Thermal Processes, 4th edition.* John Wiley & Sons, Hoboken, NJ.

[7] Durão, B., Joyce, A., Farinha Mendes, J. (2014). "Optimization of a seasonal storage solar system using Genetic Algorithms". Solar Energy, **Vol. 101**, pp. 160–166.

[8] Eicker, U. (2014). *Energy Efficient Buildings with Solar and Geothermal Resources*. John Wiley & Sons Ltd., Chichester, UK. ISBN 9781118352243.

[9] Han, Y.M., Wang, R.Z., and Dai, Y.J. (2009). "Thermal stratification within the water tank". *Renewable and Sustainable Energy Reviews*, **Vol. 13**, pp. 1014–1026. doi:10.1016/j.rser.2008.03.001

[10] Holth, E. (2009). Model Predictive Control of mixed solar and electric heating. MSc thesis, NTNU, Norway.

[11] Jordan, U., and Vajen, K. (2000). "Influence of the DHW load profile on the fractional energy savings: a case study of a solar combi-system with trnsys simulations". Solar Energy, **Vol. 69**, Nos. 1–6, pp. 197-208.

[12] Kratzenberg, M.G., Beyer, H.G., and Colle, S. (2006). "Uncertainty calculation applied to different regression methods in the quasi-dynamic collector test". Solar Energy, **Vol. 80**, pp. 1453–1462

[13] Perera., D.W.U., Pfeiffer, C., and Skeie, N.-O. (2014). "Modelling the heat dynamics of a residential building unit: Application to Norwegian buildings". *Modeling, Identication and Control*, **Vol. 35**, No. 1, pp. 43–57, ISSN 1890-1328. doi:10.4173/mic.2014.1.4.

[14] Perera., D.W.U., Pfeiffer, C., and Skeie, N.-O. (2014). "Modeling and simulation of multi zone buildings for better control". *Proceedings, SIMS 2014, Aalborg, Denmark, October 21–22, 2014*.

[15] Pichler, M.F., Lerch, W., Heinz, A., Goertler, G., Schranzhofer, H., Rieberer, R. (2014). "A novel linear predictive control approach for auxiliary energy supply to a solar thermal combistorage". Solar Energy, **Vol. 101**, pp. 203–219.

[16] Powell , K.M., and Edgar, T.F. (2012). "Modeling and control of a solar thermal power plant with thermal energy storage". Chemical Engineering Science, **Vol. 71**, pp. 138–145.

[17] Powell , K.M., and Edgar, T.F. (2013). "An adaptive-grid model for dynamic simulation of thermocline thermal energy storage systems". *Energy Conversion and Management,* **Vol. 76**, pp. 865–873. http://dx.doi.org/10.1016/j.enconman.2013.08.043.

[18] Saleh, A.M. (2012). *Modeling of Flat-Plate Solar Collector Operation in Transient States*. M.Sc. thesis, Purdue University, Indiana.

[19] Zima, W., and Dziewa, P. (2010). "Mathematical modelling of heat transfer in liquid flat-plate solar collector tubes". Archives of Thermodynamics, **Vol. 31**, No. 2, pp. 45—62. doi: 10.2478/v10173-010-0008-7.